

PAPER

## Transparent thermoplastic polyurethane air filters for efficient electrostatic capture of particulate matter pollutants

To cite this article: Ruowang Chen *et al* 2019 *Nanotechnology* **30** 015703

View the [article online](#) for updates and enhancements.



**IOP | ebooks™**

Bringing you innovative digital publishing with leading voices to create your essential collection of books in STEM research.

Start exploring the collection - download the first chapter of every title for free.

# Transparent thermoplastic polyurethane air filters for efficient electrostatic capture of particulate matter pollutants

Ruowang Chen<sup>1</sup>, Xiaowei Zhang<sup>1,2,5</sup> , Pengjun Wang<sup>1,3,5</sup>, Kaihe Xie<sup>1</sup>, Jiawen Jian<sup>1</sup>, Yuejun Zhang<sup>1</sup>, Jingrong Zhang<sup>1</sup>, Yulian Yuan<sup>1</sup>, Pudan Na<sup>1</sup>, Mingqiang Yi<sup>4</sup> and Jun Xu<sup>2</sup> 

<sup>1</sup> Department of Electrical Engineering and Computer Science, Ningbo University, Ningbo, 315211, People's Republic of China

<sup>2</sup> National Laboratory of Solid State Microstructures, Collaborative Innovation Center of Advanced Microstructures, and Department of Electronic Science and Engineering, Nanjing University, Nanjing, 210093, People's Republic of China

<sup>3</sup> College of Mathematical, Physics and Electronic Information Engineering, Wenzhou University, Wenzhou, 325035, People's Republic of China

<sup>4</sup> Microfluidic Foundry LLC, San Pablo, CA, 94806, United States of America

E-mail: [zhangxiaowei@nbu.edu.cn](mailto:zhangxiaowei@nbu.edu.cn) and [wangpengjun@nbu.edu.cn](mailto:wangpengjun@nbu.edu.cn)

Received 10 August 2018, revised 27 September 2018

Accepted for publication 3 October 2018

Published 25 October 2018



CrossMark

## Abstract

Particulate matter (PM) air pollution has been established as a significant threat to public health and a destructive factor to the climate and eco-systems. In order to eliminate the effects of PM air pollution, various air filtering strategies based on electrospun nanofibers have recently been developed. However, to date, almost none of the existing nanofibers based air filters can meet the requirements of high-performance air PM filtering, including high PM removal efficiency, low resistance to airflow, and long service life, etc. For the first time, we report a fabrication process using the electrospinning method for air filters based on thermoplastic polyurethane (TPU) nanofibers. The average diameters of TPU nanofibers are tunable from  $0.14 \pm 0.06 \mu\text{m}$  to  $0.82 \pm 0.22 \mu\text{m}$  by changing the TPU concentrations in polymeric solutions. The optimized TPU nanofibers based air filters demonstrate the attractive attributes of high  $\text{PM}_{2.5}$  removal efficiency up to 98.92%, good optical transparency of  $\sim 60\%$ , low pressure drop of  $\sim 10 \text{ Pa}$ , high quality factor of  $0.45 \text{ Pa}^{-1}$ , and long service life under the flow rate of  $200 \text{ ml min}^{-1}$ , which is ground-breaking compared with the existing nanofibers based air filters. These TPU nanofibers based air filters, with the excellent filtration performance and light transmittance, will shed light on the future research of nanofibers for various filtration applications and greatly benefit the public health by reducing the effects of PM air pollution.

Supplementary material for this article is available [online](#)

Keywords: TPU nanofiber, particulate matter, air filter, removal efficiency, pressure drop

(Some figures may appear in colour only in the online journal)

## 1. Introduction

With the rapid economic growth and increased urbanization, airborne particulate matter (PM) is causing more and more serious air pollution and threatening the public health [1]. On

<sup>5</sup> Authors to whom any correspondence should be addressed.

the basis of the particle size, PM is categorized as  $PM_{2.5}$  and  $PM_{10}$ , which refers to particles with an aerodynamic diameter of less than or equal to  $2.5 \mu\text{m}$  and  $10 \mu\text{m}$ , respectively. In particular,  $PM_{2.5}$  is more hazardous since it can directly be inhaled into parts of the lung through human nose and bronchi [2–4]. Long-term exposure to  $PM_{2.5}$  pollutants may result in many diseases, including asthma, pulmonary fibrosis, cancer, chronic obstructive pulmonary disease, type-2 diabetes and even cardiovascular diseases [5, 6]. These  $PM_{2.5}$  pollutants are mainly produced by industrial coal use and fossil fuel combustion. Over the past decade,  $PM_{2.5}$  air pollution problems have become progressively worse, especially in the major developing countries, including India and China [7]. To reduce the effects of  $PM_{2.5}$  air pollution, many air filtering strategies based on electrospun nanofibers have been adopted in window purification filters for indoor air-quality protection or in mask filters for outdoor individual protection [8–10]. However, up to now, the overall performance of existing fibrous  $PM_{2.5}$  air filters, including the  $PM_{2.5}$  removal efficiency, pressure drop, quality factor ( $QF$ ), and service life, can rarely meet the requirement of high-performance air filters. The core part of these  $PM_{2.5}$  air filters is the electrospun nanofibers. To improve the filtration performance of current fibrous air filters, great efforts have been made recently. A series of electrospun nanofibers, such as polyvinyl alcohol [11], polyacrylonitrile [12, 13], polyethylene terephthalate [14], polylactic acid [15], polyamide-66 [16], and polyimide [17], are fabricated and tested as the novel nanoscale building block used in the high-performance  $PM_{2.5}$  air filters. These electrospun nanofibers exhibit ultrathin diameters, extensively interconnected pores, and adjustable porosity. Despite these advantages, these  $PM_{2.5}$  air filters, based on existing electrospun nanofibers, still face the challenge of low PM removal efficiency, high airflow resistance, poor mechanical property and biocompatibility.

Compared with other electrospun nanofibers reported before, thermoplastic polyurethane (TPU) is a widely used class of polymer with high abrasion resistance, good optical transparency, high elasticity, good stability and biocompatibility [18]. In this work, air filters based on TPU nanofibers with different average diameters are fabricated by the electrospinning method and tested for the filtration performance of  $PM_{2.5}$  and  $PM_{10}$  under different airflow rates. Compared with other air filters reported before, TPU nanofibers air filters demonstrate the attractive attributes of high removal efficiency, good optical transparency, low resistance to airflow, and relatively long service life. By controlling the average diameters of TPU nanofibers precisely, we report the optimal TPU air filters with 98.92% removal of  $PM_{2.5}$ ,  $\sim 10$  Pa pressure drop,  $0.45 \text{ Pa}^{-1} QF$ ,  $\sim 60\%$  transparency, and long service life under a flow rate of  $200 \text{ ml min}^{-1}$ . We anticipate that these TPU nanofibers based air filters, with the excellent filtration performance and good biocompatibility, will greatly benefit the public health in reducing the effects of  $PM_{2.5}$  air pollution.

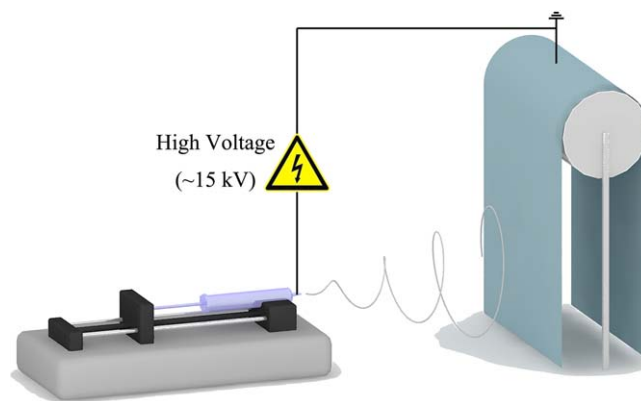


**Figure 1.** Schematic diagram of the set-up of electrospinning apparatus for the fabrication of TPU nanofibers by the electrospinning process.

## 2. Experiment

TPU polymer (Elastollan, 1185A) was obtained from BASF Co., Ltd. *N, N*-Dimethylformamide (DMF) and acetone were purchased from the Macklin Biochemical Co., Ltd. All chemicals and solvents were used as received. Electrospinning solutions were prepared by dissolving the different TPU concentrations in the mixed solvent with DMF and acetone at a volume ratio of 1:1. To ensure the homogeneous dispersion and complete dissolving of TPU, the ultrasonic dispersion method was employed for 10 min at room temperature. The electrospinning process was performed by use of a homemade spinning machine and the conceptual illustration of the electrospinning process is displayed in figure 1. The polymer solution was loaded in a syringe with a 22G needle tip, which was connected to a voltage supply device (model DW-P503-1ACF0). The electrospinning solution was pumped out of the needle tip by use of a syringe pump (model LSP01-1A). The fiber glass wire mesh substrate was sputter-coated with 150 nm of copper on both sides and was grounded to collect the electrospinning TPU nanofibers. The diameter of the fiber glass wire was 3.35 mm and the mesh substrate was cut into pieces with size of  $90 \text{ mm} \times 90 \text{ mm}$  for the PM filtration performance measurements. During the electrospinning process, the electrospun nanofibers lay across the mesh hole to form the fibrous air filter membrane, similar to previous reports [19, 20]. The applied potential between the needle tip and the collector was fixed at 15 kV, the tip-to-collector distance was kept at 12 cm, and the TPU solution feeding rate was kept at  $0.9 \text{ ml h}^{-1}$  during the electrospinning process. The TPU concentrations in solution were adjusted from 8 wt% to 18 wt% to control the average diameter of the nanofibers. The formation of TPU nanofibers with different average diameters was confirmed by a scanning electron microscope (SEM, model Hitachi S-400) with an acceleration voltage of 5 kV. The ambient temperature was  $20 \text{ }^\circ\text{C} \pm 5 \text{ }^\circ\text{C}$  and humidity was 48%–52% during the electrospinning process.

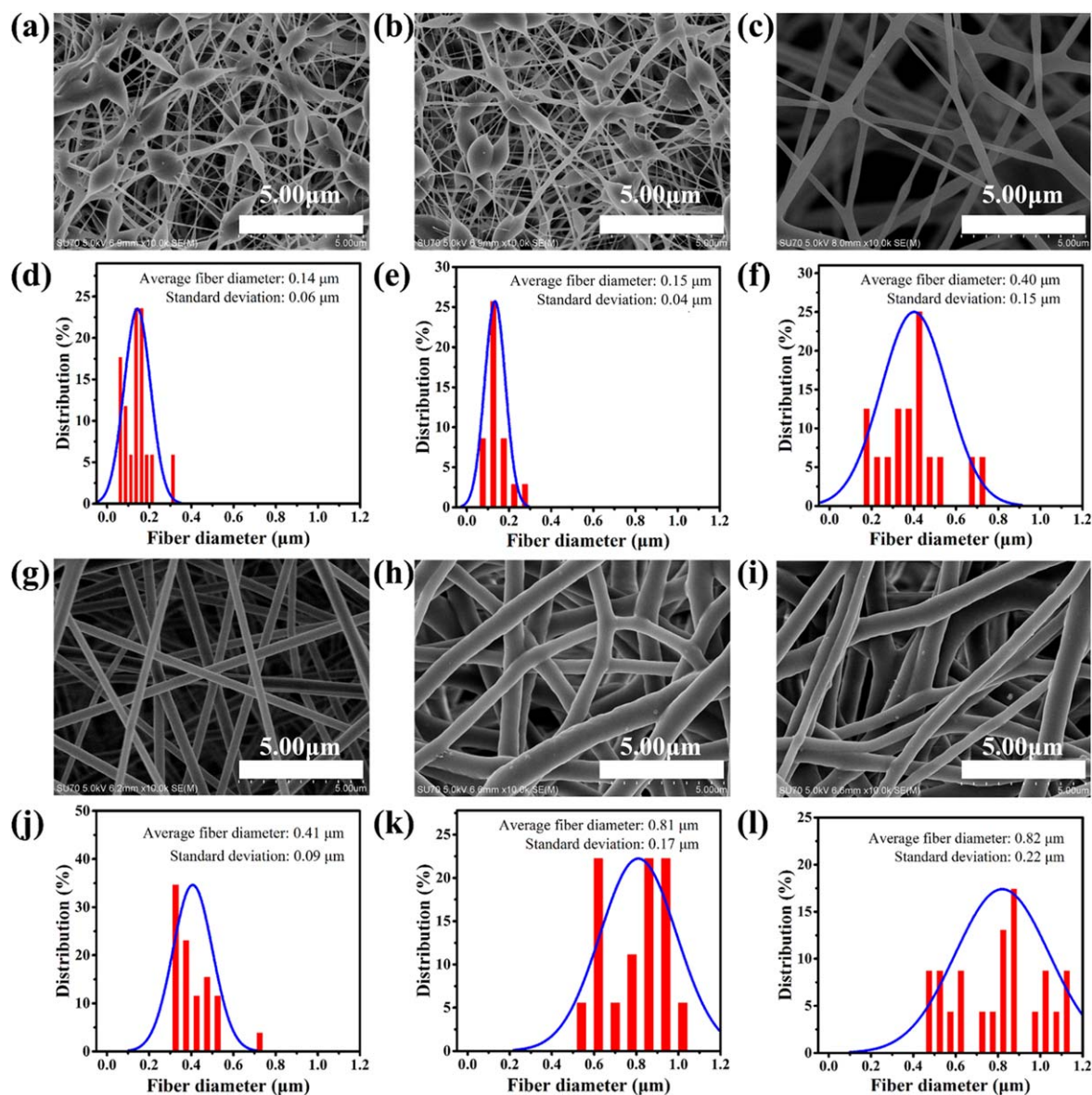


**Figure 2.** (a)–(c), (g)–(i) SEM images of the nanofiber membranes obtained from solutions with TPU concentrations of 8 wt%, 10 wt%, 12 wt%, 14 wt%, 16 wt%, 18 wt%, respectively. (d)–(f), (j)–(l) The TPU nanofibers diameter distributions corresponding to (a)–(c) and (g)–(i), respectively.

### 3. Results and discussion

As shown in figures 2(a)–(c) and (g)–(i), the typical morphologies of electrospun TPU nanofibers are presented under different TPU concentrations of 8 wt%, 10 wt%, 12 wt%, 14 wt%, 16 wt%, 18 wt%, respectively. When the TPU concentration is below 12 wt% in precursor, it is clear that many bead-like nanofibers as well as connecting sites are formed randomly. It can be explained as the viscoelasticity of polymer TPU molecular chains. During the electrospinning process, the jet from precursors with low TPU concentrations is hard to effectively resist the stretching from the electric field force [21]. Then, the molecular chains will agglomerate to form bead-like nanofibers because of the viscoelasticity of polymer TPU molecular chains [22]. With the increasing TPU concentrations in precursors, the number density of bead-like nanofibers decreases and the connecting sites, such

as crossing and bonding sites, will totally disappear. Meanwhile, the average diameter of TPU nanofibers increases quickly when the TPU concentration is above 12 wt%. The diameter distribution analysis is performed by the ImageJ software. Digital high-resolution SEM images are firstly converted to binary images and then the average nanofiber diameter and the diameter distribution are determined by counting pixels of each discrete TPU nanofiber. As shown in figures 2(d)–(f) and (j)–(l), the average nanofiber diameter is  $0.14 \pm 0.06 \mu\text{m}$ ,  $0.15 \pm 0.04 \mu\text{m}$ ,  $0.40 \pm 0.15 \mu\text{m}$ ,  $0.41 \pm 0.09 \mu\text{m}$ ,  $0.81 \pm 0.17 \mu\text{m}$ , and  $0.82 \pm 0.22 \mu\text{m}$ , corresponding to the TPU concentrations from 8 wt% to 18 wt% in precursors, respectively.

The  $\text{PM}_{2.5}$  filtration performance of TPU nanofibers based air filters is evaluated in a text box containing two chambers at room temperature. The PM pollutants are generated by the burning of cigarettes in one chamber and the TPU nanofibers

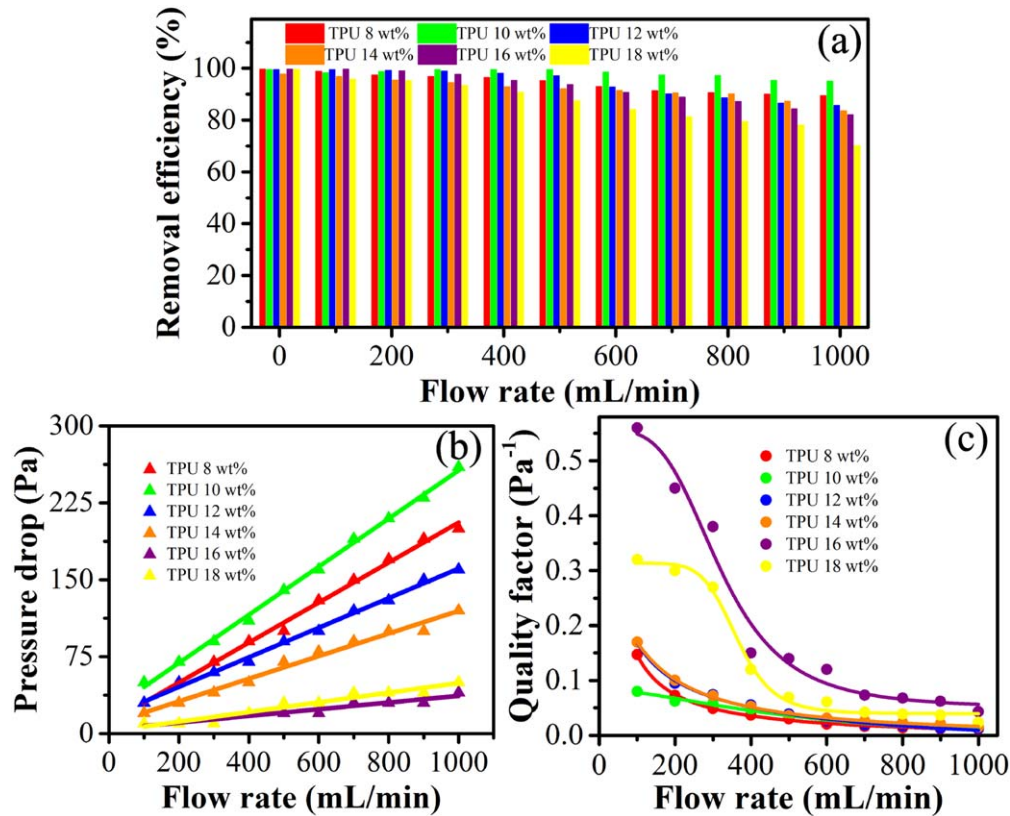


**Figure 3.** (a)  $PM_{2.5}$  removal efficiency, (b) pressure drop, and (c) quality factor of air filters fabricated from electrospinning solution with TPU concentrations from 8 wt% to 18 wt% under the different airflow rates.

based air filters are used to block the PM dispersion into the other chamber. The size of smoke PM used here mainly distributes less than  $1 \mu m$  and the concentration of smoke PM in the pollution area is maintained at a level of  $>350 \mu g \cdot m^{-3}$ . The number concentrations of smoke PM at two areas are measured by the standardized particle detectors. The removal efficiency is calculated by comparing the number concentrations before and after filtration. Figure 3(a) shows the  $PM_{2.5}$  removal efficiency of air filters under various airflow rates. It is worth mentioning that the highest removal efficiency reaches 99.64% under the condition of no airflow. With the increasing airflow rate, the  $PM_{2.5}$  removal efficiencies of all TPU nanofibers based air filters decrease slightly. At the same airflow rate, the removal efficiency is improved with the increasing TPU concentrations from 8 wt% to 10 wt%, which can be ascribed to the fact that the nanofibers with larger diameters resist PM particle spread more easily. On the other hand, with TPU concentrations increasing from 10 wt% to 18 wt%, the disappearance of connecting sites and bead-like nanofibers, and the increasing interspace between TPU nanofibers, make the removal efficiency decrease obviously. Figure 3(b) compares the pressure drops of air filters under different airflow rates. The pressure drop exhibits an increased trend directly proportional to the flow rate, which obeys the Darcy's theory very well. Meanwhile, it is found that the pressure drop first increases, then keeps falling and finally increases slightly, corresponding to air filters with the TPU concentration

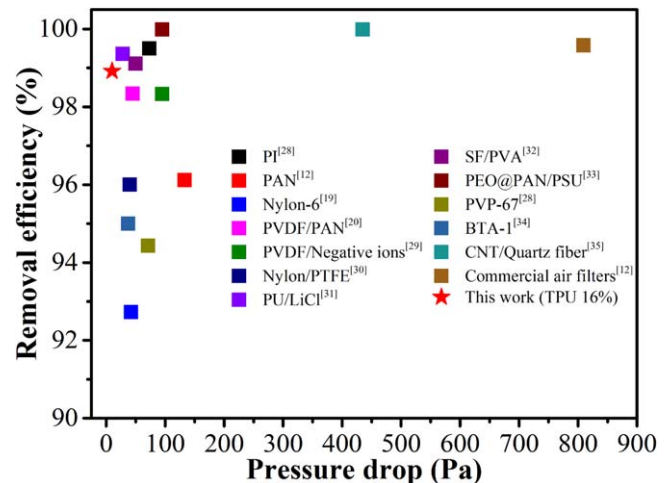


**Figure 4.** Performance summary of air filters fabricated from different materials in recent literatures. PVDF stands for polyvinylidene fluoride. SF stands for silk fibroin. PEO stands for plasma electrolytic oxidation. PSU stands for polysulfide. PVP stands for polyvinyl pyrrolidone. BTA-1 stands for 1, 3, 5-benzenetricarboxamide. CNT stands for carbon nanotube.

increasing from 8 wt% to 10 wt%, 10 wt% to 16 wt% and 16 wt% to 18 wt% at the same flow rate. According to previous reports [23–25], we consider that there exist two factors influencing the pressure drop, nanofiber diameter and the

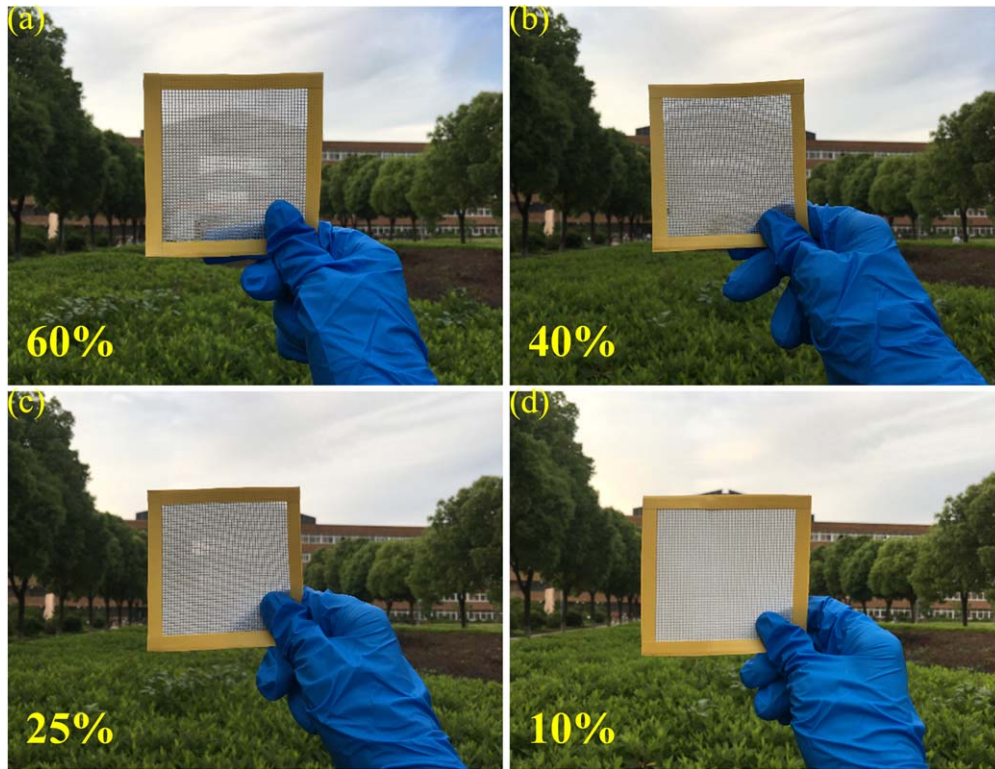


**Figure 5.** Photographs of TPU nanofibers based air filters fabricated from electrospinning on the fiber glass wire mesh with an electrospinning time of (a) 10 min, (b) 20 min, (c) 30 min, (d) 40 min, respectively.

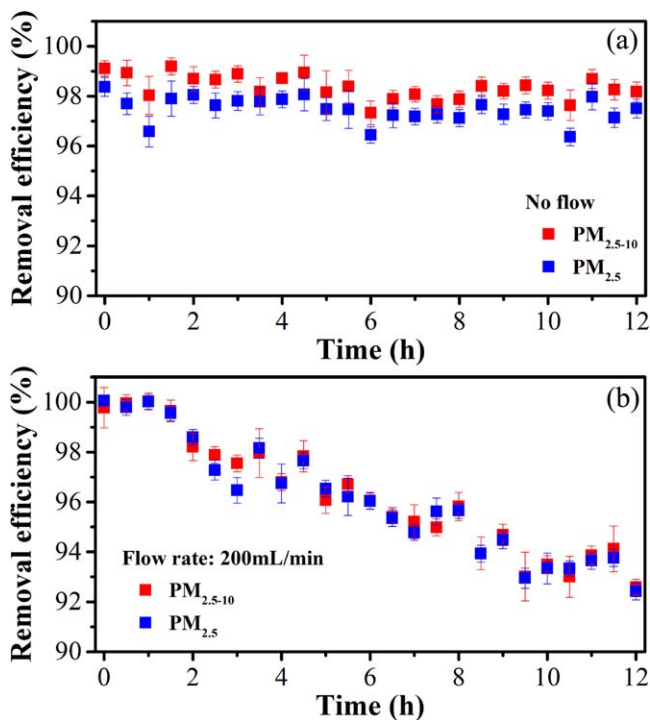


**Figure 6.** The long-term  $PM_{2.5-10}$  and  $PM_{2.5}$  removal efficiencies of the TPU air filter with 60% transmittance under a continuously hazardous level of PM pollution with (a) no airflow, (b) airflow rate of  $200 \text{ ml min}^{-1}$ . Error bar represents the standard deviation of three replicate measurements.

nanofiber packing density. The nanofiber packing density is defined as follows,

$$\alpha = \frac{W}{\rho_f Z}, \quad (1)$$

where  $\alpha$  stands for the nanofiber packing density,  $W$  is the mass of nanofibers per unit filter area,  $\rho_f$  is the density of nanofibers, and  $Z$  is the thickness of nanofibers. The initial increase in pressure drop is mainly attributed to the increase of TPU nanofiber average diameters. With the increasing TPU concentrations from 10 wt% to 16 wt%, the decrease of nanofiber packing density enlarges the interspace between nanofibers, which benefits more effective air permeability, although the average thickness of the nanofiber is further increased. When an air filter fabricated from solutions with a TPU concentration of 18 wt% nanofiber diameter plays a more significant role in air resistance than the nanofiber, packing density and the related pressure drop increases slightly. A trade-off parameter, named  $QF$ , is introduced to evaluate filtration capacity of the air filters based on the PM removal efficiency and related pressure drop. The values of  $QF$  can be defined by the following formula [26, 27],

$$QF = -\frac{\ln(1 - \eta)}{\Delta p}, \quad (2)$$

where  $\eta$  stands for the removal efficiency and  $\Delta p$  stands for the pressure drop before and after filtration. Figure 3(c) shows the  $QFs$  of air filters fabricated from electrospinning solution with

different TPU concentrations from 8 wt% to 18 wt%. Obviously, with the increasing flow rate from 100 ml min<sup>-1</sup> to 1000 ml min<sup>-1</sup>, the values of  $QF$ s decrease because of the rapidly increasing PM treatment capacity. When the TPU concentration is 16 wt%, the  $QF$  of the air filter reaches 0.45 Pa<sup>-1</sup>, where the PM<sub>2.5</sub> removal efficiency is 98.92% and the related pressure drop is only 10 Pa at the flow rate of 200 ml min<sup>-1</sup>. In comparison with the available literatures [28–35], as shown in figure 4, our TPU air filter exhibits highly improved filtration performance achieved by the largest  $QF$  value. Besides the TPU concentrations in precursor, note that other processing parameters, such as the applied voltage and tip-to-collector distance, can influence the average diameter and morphology of TPU nanofibers during the electrospinning process [36, 37]. The PM<sub>2.5</sub> removal efficiency, pressure drop, and the related quality factor values of TPU nanofibers based air filters fabricated from the different applied voltages and tip-to-collector distances are demonstrated, as shown in figures S1 and S2, available online at [stacks.iop.org/NANO/30/015703/mmedia](https://stacks.iop.org/NANO/30/015703/mmedia) (supporting information 1).

Further, the visible light transmittance of the TPU air filter is investigated by use of an optical transmittance meter. Figures 5(a)–(d) show the photographs of a TPU nanofibers based air filter with electrospinning times of 10 min, 20 min, 30 min, and 40 min, corresponding to the visible light transmittance of ~60%, ~40%, ~25%, ~10%, respectively. Detailed measuring processes are depicted in supporting information 2. For the optimal TPU air filters, with a transmittance above 50%, the sufficient sunlight can penetrate through TPU nanofibers. Therefore, the material use for the TPU nanofibers based air filters can be reduced significantly to a transparent level. Besides, this good optical transparency can make the TPU nanofibers based air filters be applied to all types of situations, including building windows for indoor air-quality protection. We anticipate that there are no fundamental obstacles to extending these new TPU nanofibers to PM filtrations, and these TPU nanofibers based air filters will be a starting point for future high-efficiency and durable PM filters, with good optical transparency and biocompatibility.

Besides, the long-term PM<sub>2.5</sub> and PM<sub>2.5-10</sub> removal efficiencies of a TPU air filter with 60% transmittance are studied, as shown in figures 6(a) and (b). The PM<sub>2.5</sub> and PM<sub>2.5-10</sub> removal efficiencies under no airflow are still kept at >96% and >97% within a test time of 12 h, respectively. The PM<sub>2.5-10</sub> removal efficiency is always slightly higher than PM<sub>2.5</sub> under no airflow, indicating that the natural diffusion ability of PM<sub>2.5-10</sub> is even worse than PM<sub>2.5</sub>. When airflow rate is adjusted at 200 ml min<sup>-1</sup>, both PM<sub>2.5</sub> and PM<sub>2.5-10</sub> removal efficiencies are >92% within the test time of 12 h. Before and after filtration testing, the morphologies of TPU nanofibers air filters are compared according to the SEM images, as shown in figure S3 (supporting information 3). We predict that both PM<sub>2.5</sub> and PM<sub>2.5-10</sub> removal efficiencies will become worse with a larger flow rate above 1000 ml min<sup>-1</sup>. For the transparent TPU nanofibers based air filters, under the larger flow rate condition, the longer term effective particles capture is a question that needs careful consideration in the future.

## 4. Conclusion

In summary, the electrospinning method for the fabrication of air filters based on TPU nanofibers with different diameters is reported for the first time. Under the airflow rate of 200 ml min<sup>-1</sup>, the optimal TPU nanofibers based air filters show the high PM<sub>2.5</sub> removal efficiency up to 98.92%, good optical transparency of ~60%, low pressure drop of ~10 Pa, high quality factor of 0.45 Pa<sup>-1</sup>, and long service life. The breakthroughs of above performance improvements enable the air PM filtering by the nanofibers based devices, paving the way for the commercial application of these technologies. With the excellent filtration performance, such TPU nanofibers based air filters will not only lighten the future research on various nanofibers based air filters, but also enable their commercialization in filtering air PM and greatly benefit public health.

## Acknowledgments

This work was supported by the National Natural Science Foundation of China (NSFC) (61704094, 61735008, 11774155, 61471210 and 61474068), the Program 973 (2013CB632101), the Research Foundation of Education Bureau of Zhejiang Province (Y201737316), and the K C Wong Magna Fund in Ningbo University. We also expressed special thanks to Dr Paul Lum from the Bio-molecular Nano Center at University of California at Berkeley, for the fabrication and filtration measurements of various TPU nanofibers based air filters.

## ORCID iDs

Xiaowei Zhang  <https://orcid.org/0000-0001-7443-0562>  
Jun Xu  <https://orcid.org/0000-0002-0469-9766>

## References

- [1] Kelly F J and Zhu T 2016 *Science* **352** 934–6
- [2] Mahowald N 2011 *Science* **334** 794–6
- [3] Zhang X, Zhang W, Yi M, Wang Y, Wang P, Xu J, Niu F and Lin F 2018 *Sci. Rep.* **8** 4757
- [4] Zhu L *et al* 2017 *Environ. Sci. Technol.* **51** 5650–7
- [5] Zhang S, Wolf K, Breiter S, Kronenberg F, Stafoggia M, Peters A and Schneider A 2018 *Environ. Int.* **118** 17–25
- [6] Ngo N S, Bao X J and Zhong N 2018 *Environ. Res.* **165** 473–83
- [7] Maji K J, Dikshit A K, Arora M and Deshpande A 2018 *Sci. Total Environ.* **612** 683–93
- [8] Khalid B, Bai X, Wei H, Huang Y, Wu H and Cui Y 2017 *Nano Lett.* **17** 1140–8
- [9] Yang A, Cai L, Zhang R, Wang J, Hsu P, Wang H, Zhou G, Xu J and Cui Y 2017 *Nano Lett.* **17** 3506–10
- [10] Zhang Y, Yuan S, Feng X, Li H, Zhou J and Wang B 2016 *J. Am. Chem. Soc.* **138** 5785–8
- [11] Kong C S, Yoo W S, Lee K Y and Kim H S 2009 *J. Mater. Sci.* **44** 1107–12

- [12] Liu C, Hsu P C, Lee H W, Ye M, Zheng G, Liu N, Li W and Cui Y 2015 *Nat. Commun.* **6** 6205
- [13] Su S, Li J L, Zhou L, Wan S, Bi H C, Ma Q and Sun L T 2017 *J. Nano. Res.* **46** 73–81
- [14] Bahners T, Molter-Siemens W, Haep S and Gutmann J S 2014 *Appl. Surf. Sci.* **313** 93–101
- [15] Wang Z, Zhao C and Pan Z 2015 *J. Colloid Interface Sci.* **441** 121–9
- [16] Shahrabi S, Gharehaghaji A A and Latifi M 2016 *J. Ind. Text* **45** 1100–14
- [17] Gu G, Han C, Lu C, He C, Jiang T, Gao Z, Li C and Wang Z 2017 *ACS Nano* **11** 6211–7
- [18] Polat Y, Pampal E S, Stojanovska E, Simsek R, Hassanin A, Kilic A, Demir A and Yilmaz S 2016 *J. Appl. Polym. Sci.* **133** 43025
- [19] Xu J, Liu C, Hsu P C, Liu K, Zhang R, Liu Y and Cui Y 2016 *Nano Lett.* **16** 1270–5
- [20] Zhao X, Li Y, Hua T, Jiang P, Yin X, Yu J and Ding B 2017 *Small* **13** 1603306
- [21] Fong H, Chun I and Reneker D H 1999 *Polymer* **40** 4585–92
- [22] Sun M, Li X, Ding B, Yu J and Sun G 2010 *J. Colloid Interface Sci.* **347** 147–52
- [23] Leung W W F, Hung C H and Yuan P 2010 *Sep. Purif. Technol.* **71** 30–7
- [24] Wang C and Otani Y 2013 *Ind. Eng. Chem. Res.* **52** 5–17
- [25] Wan L Y Q, Wang H, Gao W and Ko F 2015 *Polymer* **73** 62–7
- [26] Chen C Y 1955 *Chem. Rev.* **55** 595–623
- [27] Li P, Wang C, Zhang Y and Wei E 2014 *Small* **10** 4543–61
- [28] Zhang R et al 2016 *Nano Lett.* **16** 3642–9
- [29] Zhao X, Li Y, Hua T, Jiang P, Yin X, Yu J and Ding B 2017 *ACS Appl. Mater. Interfaces* **9** 12054–63
- [30] Bai Y, Han C, He C, Gu G, Nie J, Shao J, Xiao T, Deng C and Wang Z 2018 *Adv. Funct. Mater.* **28** 1706680
- [31] Zuo F, Zhang S, Liu H, Fong H, Yin X, Yu J and Ding B 2017 *Small* **13** 1702139
- [32] Bian Y, Wang R, Ting S, Chen C and Zhang L 2018 *IEEE Trans. Nanotechnol.* **5** 934–9
- [33] Zhang S, Liu H, Yin X, Yu J and Ding B 2016 *ACS Appl. Mater. Interfaces* **8** 8086–95
- [34] Weiss D, Skrybeck D, Misslitz H, Nardini D, Kern A, Kreger K and Schmidt H W 2016 *ACS Appl. Mater. Interfaces* **8** 14885–92
- [35] Li P, Wang C, Li Z, Zong Y, Zhang Y, Yang X, Li S and Wei F 2014 *RSC Adv.* **4** 54115–21
- [36] Xue J, Xie J, Liu W and Xia Y 2017 *Acc. Chem. Res.* **50** 1976–87
- [37] Kenry and Lim C T 2017 *Prog. Polym. Sci.* **70** 1–17